Technical Report

Corrosion characteristic of Ce Al brass in comparison with As Al brass

J.L. Chen [a], Z. Li [a,b,*], Y.Y. Zhao [b]

[a] School of Materials Science and Engineering, Central South University, Changsha 410083, China
[b] Department of Engineering, University of Liverpool, Liverpool L69 3GH, UK

ARTICLE INFO

ABSTRACT

An Al brass alloy with Ce addition has been developed with an aim to replace the As Al brass, because the latter poses health and environmental problems. The corrosion behavior of the two alloys in NaCl (35 g/L) and NaCl (35 g/L) + NH$_4$Cl (26.75 g/L) solutions has been investigated. The morphology and compositional changes in the alloys have been studied. In both solutions, the corrosion rates of the Ce Al brass are very similar to those of As Al brass. Ce is a suitable alternative to As as an alloying element in Al brass for corrosion resistance improvement.

© 2008 Elsevier Ltd. All rights reserved.

1. Introduction

Copper-based alloys are widely used in marine environments, due to their excellent electrical and thermal conductivity, good corrosion resistance and ease of manufacture. Brass alloys have wide industrial applications as condensers and heat exchanger systems in saline water [1]. Pitting corrosion [2], dezincification [3,4] and stress corrosion cracking [5,6] of brass in water have been widely studied. Dealloying, or dezincification, in brass may be readily observed with naked eyes because the alloy develops a reddish color that contrasts with its original yellowish color. Generally, there are two types of dealloying. Uniform or layer dealloying commonly occurs in high zinc alloys where the outer layer is dealloyed and becomes dark while the inside is not affected; plug dealloying is typified by the presence of the dealloyed dark plugs in the unaffected matrix of low zinc alloys [7–11]. Two theories have been proposed for dealloying of brass. One states that there is anodic dissolution of the brass (both copper and zinc) while the copper ions plate back from the solution on the remaining brass surface as a porous layer; the other states that the less noble alloying elements are selectively dissolved, leaving vacancies in the brass lattice structure resulting in skeletal copper with poor mechanical integrity [12].

In the past decade, many alloying elements have been used to minimize the dezincification and corrosion of brass alloys. In particular, arsenic (As) has been added into several conventional brass alloys, such as H68, HSn70-1 and HAl77-2 because it can inhibit the dezincification of brass effectively [13,14]. Since As can pose health and environmental problems, however, there is a need to find suitable alternatives which can improve the corrosion

resistance of brass alloys. Rare-earth elements are potential substitutes for As [15].

In the present work, a new aluminum (Al) brass alloy with cerium (Ce) and boron (B) additions has been developed with an aim to replace for the As Al brass. In order to study the feasibility of Ce as an alternative to As in Al brass, the corrosion behavior of the Ce Al brass and that of the As Al brass has been studied by corrosion tests and microscopic analysis.

2. Experimental procedures

Two Al brass alloys were prepared by induction melting and mold casting. Their compositions are shown in Table 1. The surface defects of the ingots, surface inclusion and surface oxide, were first removed by mechanical milling. The ingots were then homogenized at 1023 K for 2 h and subsequently rolled from a thickness of 22 mm into strips of 2 mm thick. The strips were annealed at 837 K for 1 h. Specimens with dimensions of $1.8 \times 20 \times 40$ mm were cut from the strips and mechanically polished with glazing machine.

The specimens were immersed into either NaCl (35 g/L) or NaCl (35 g/L) + NH$_4$Cl (26.75 g/L) solutions for 30 days and the corrosion products on the specimens were then removed by 1:1 hydrochloric acid solution. The weights of the specimen both before and after the corrosion tests were measured by TG328A analytical balance with accurate of 0.1 mg. The corrosion rate of the specimen, R (mm/yr), was determined by

$$R = \frac{m - (m_t + m_o)}{\rho S t} \tag{1}$$

where m (g) is the weight of the specimen before corrosion, m_t (g) is the weight of the specimen after corrosion, m_o (g) is the weight loss of a non-corroded specimen immersed in the 1:1 hydrochloric acid solution, ρ (g/mm^3) is the density of specimen, S (mm^2) is the

* Corresponding author. Address: School of Materials Science and Engineering, Central South University, Changsha 410083, China. Tel.: +86 731 8830264; fax: +86 731 8876692.
E-mail addresses: lizhou6931@gmail.com, lizhou6931@163.com (Z. Li).

Table 1
The compositions of the As and Ce Al brass alloys

	Alloying elements (wt%)							
	Cu	Al	Fe	Ni	As	B	Ce	Zn
As Al brass	77	2.2	0.06	1.0	0.06	0.010	None	Balance
Ce Al brass	77	2.2	0.06	1.0	None	0.010	0.01	Balance

surface area of the specimen, and $t = 0.0833$ yr is the time that the specimen was immersed in the solution. Besides corrosion products were removed by hydrochloric acid solution, non-corroded matrix alloy was removed, therefore the weight loss of a non-corroded specimen (m_o) immersed in hydrochloric acid solution should be measured to correct the corrosion rate of the specimen (R).

The electrochemical analysis of the alloys was conducted by a SI1287 electrochemical workstation with a speed of 2 mv/s, using Pt as the auxiliary electrode and the saturated calomel electrode (SCE) as the reference electrode. The CorrView software, Version 2.8d, was used to analyze the data.

Scanning electron microscopy (SEM) and energy dispersive X-ray analysis (EDAX) were preformed to characterize the corrosion products, using a Sirion200 field emission SEM equipped with EDAX GENESIS 60.

3. Results and discussion

The two alloys are hot-rolled between 973 and 1023 K, no flaw can be found in the hot-rolled plates as the reduction is to 91.6% for Ce Al brass and 90.9% for As Al brass. The Ce Al brass as cast state is cold-rolled, no flaw can be found in the cold-rolled plates as the reduction is to 60%.

Table 2 shows the average corrosion rates of the alloys in the NaCl (35 g/L) and the NaCl + NH$_4$Cl solutions. It shows that the average corrosion rates of the Ce Al brass are slightly less than those of the As Al brass.

Fig. 1 shows the polarization curves of the two alloys in the NaCl solution. Table 3 shows the characteristic parameters of the electrochemical test. R_p is polarization resistance, I_{corr} is corrosion current density and E_{corr} is corrosion potential. The corrosion potential of the Ce Al brass is lower than that of the As Al brass. However, the polarization resistance of the former is about twice as much as that of the latter, while the corrosion current density of the former is about half as much as that of the latter.

Fig. 2 shows the secondary electron (SE) SEM images of the surfaces of the As Al brass and the Ce Al brass after being immersed in the NaCl solution for 30 days. The images are representative for practically the entire surfaces of the two alloys, which are very different. The corrosion product layer of the As Al brass is porous (Fig. 2a), while that of the Ce Al brass is dense (Fig. 2b).

Fig. 3a shows the backscattered electron (BSE) SEM image of the cross-section of the As Al brass after exposure to the NaCl solution for 30 days. The corrosion product layer has a non-uniform thickness and has pores in it. The average thickness of these product layers is 2.5 μm.

There are cracks at the interface between the corrosion layer and the alloy matrix, which suggest that the bonding between the cor-
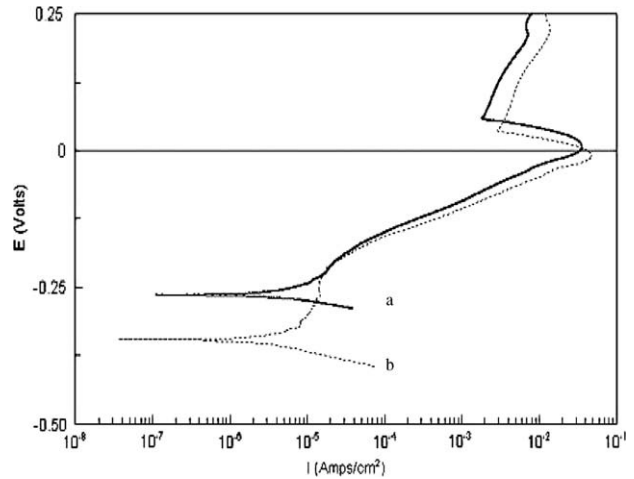
Table 2
The average corrosion rates of the As and Ce Al brass alloys

	NaCl solution (mm/yr)	NaCl + NH$_4$Cl solution (mm/yr)
As Al brass	0.007944	0.016801
Ce Al brass	0.007732	0.016798

Fig. 1. The polarization curves of (a) As Al brass and (b) Ce Al brass in the NaCl solution.

Table 3
Polarization resistance (R_p), corrosion current density (I_{corr}) and corrosion potential (E_{corr}) of the As and Ce Al brass alloys

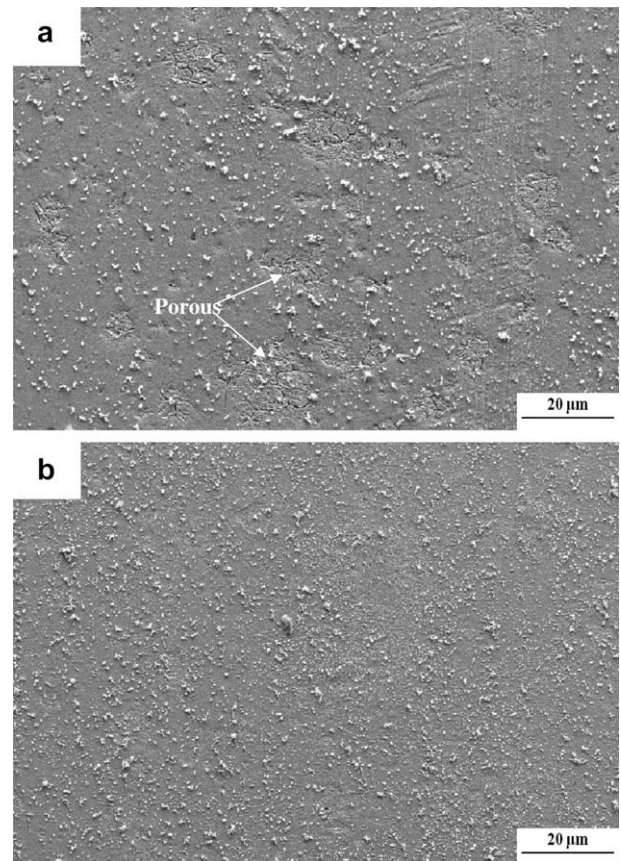|	R_p (Ω/cm^2)	I_{corr} (A/cm^2)	E_{corr} (V)
As Al brass	1387.8	1.8797E−5	−0.2638
Ce Al brass	2668.3	9.7768E−6	−0.3456

Fig. 2. SE SEM images of (a) As Al brass and (b) Ce Al brass after being immersed in the NaCl solution for 30 days.

rosion layer and the alloy matrix is weak. At certain locations, the corrosion product penetrates deeply into the matrix (see Fig. 3a).

Fig. 3. (a) SEM image and (b) EDAX line scan results of As Al brass after exposure in the NaCl solution.
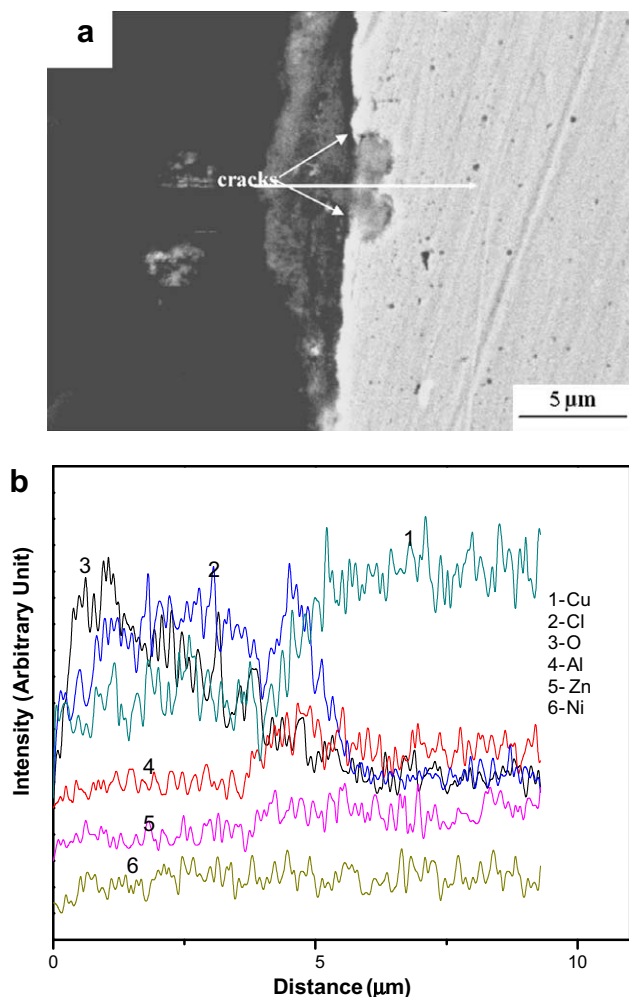

Fig. 4. (a) SEM image and (b) EDAX line scan results of Ce Al brass after exposure in the NaCl solution.

The layer has also been delaminated from the surface of the matrix at certain locations. SEM-EDX line scan was performed along the arrow in Fig. 3a and the distributions of Cu, Zn, Al, Ni, Cl and O are shown in Fig. 3b. The concentrations of Cu and Zn in the corrosion product layer are much lower than those in the matrix. That of Al in corrosion product is lower than that in the matrix, however it is higher in the interface than that in the matrix. The concentration of Ni in the layer is almost the same as that in the matrix. The concentrations of O and Cl in the corrosion product layer are much higher than those in the matrix. While the concentration of Cl stays more or less the same throughout the corrosion product layer, the concentration of O decreases steadily from the outer surface towards the matrix.

Fig. 4a shows the backscattered electron (BSE) SEM image of the cross-section of the Ce Al brass after exposure to the NaCl solution for 30 days. The corrosion product layer is dense and has a uniform thickness. The product layer adheres to the matrix and there are no apparent cracks at the interface. No localized penetration of the corrosion product into the alloy matrix is observed. There are perpendicular cracks observed in the corrosion product layer, which are caused by the forces applied during the specimen preparation. SEM-EDX line scan was performed along the arrow in Fig. 4a and the results are shown in Fig. 4b. Qualitatively, the distributions of Cu, Zn, Al, Ni, Cl and O are the same as those in Fig. 3b. However, more pronounced decreases in Cu and Zn and increases in O and Cl in the corrosion product layer are observed.
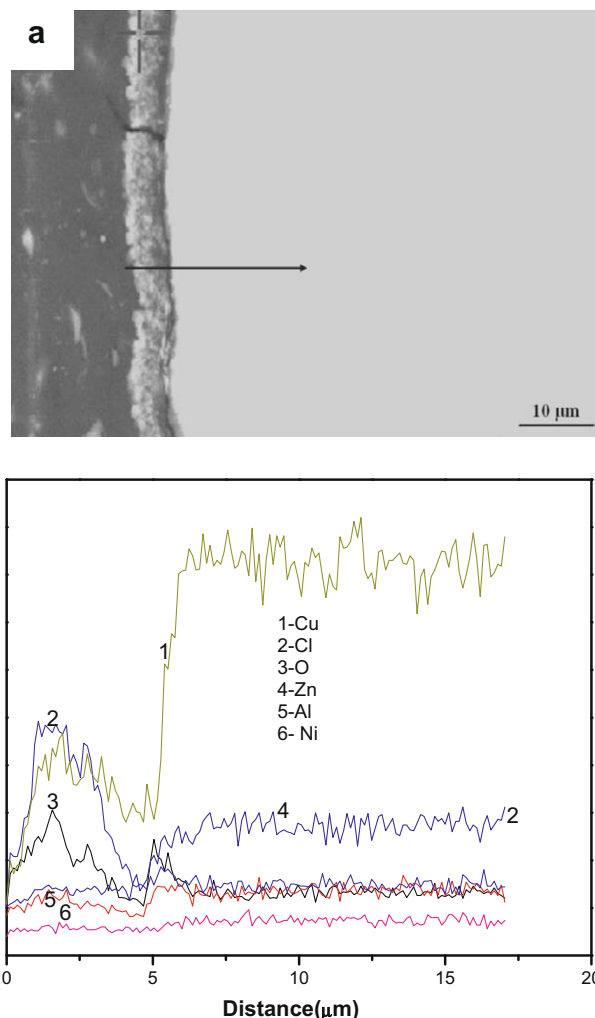
The SE SEM images of the As and the Ce Al brass alloys after exposure for 30 days in the NaCl + NH₄Cl solution are shown in Fig. 5a and b, respectively. In As Al brass, the corrosion product layer has been delaminated completely from the matrix, only can the cracks (or grain boundary) be seen on the image. In Ce Al brass, the majority of the corrosion product layer has also been delaminated from the matrix. In both cases, the grain boundaries of the alloy matrix are clearly visible.

The addition of aluminum to copper increases its corrosion resistance in sea water and salt solutions [16]. The corrosion resistance of both bronze and brass with Al content up to 8% has been attributed to a sustainable protective layer of alumina (Al_2O_3) which forms quickly on the alloy surface post-exposure to the corrosion environment [17,18]. In this study, however, the high corrosion resistance of the As Al brass cannot be attributed to this protective layer of alumina (Al_2O_3). Fig. 3b shows that the corrosion product layer is composed of Cu, Zn, Ni, O and Cl, in addition to Al. The corrosion products are likely to be a mixture of the oxides and chlorides of Al, Cu, Zn and Ni. In the corrosion product layer, there are considerable amounts of cracks and pores. The layer has also been delaminated from the surface of the matrix at certain locations. As a consequence, the protective function of the corrosion product layer is not significant.

The corrosion resistance of Al brass can be increased by the additions of As and B. The As in the brass alloys forms the "divacancy-As" duplets, which could effectively inhibit the diffusion
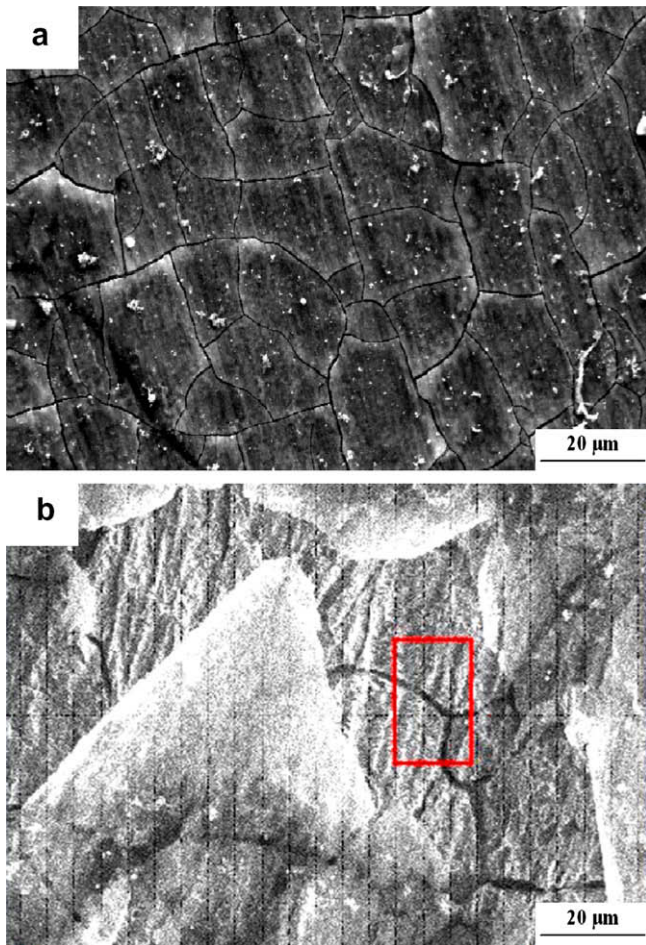
Fig. 5. SE SEM images of (a) As Al brass and (b) Ce Al brass after being immersed in the NaCl + NH$_4$Cl solution for 30 days.
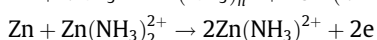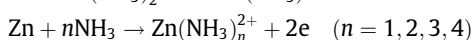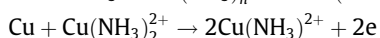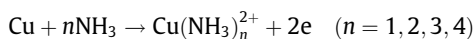
and thus the preferential solution of Zn [14]. The addition of B in the Al brass can not only refine the grains and strengthen the grain boundaries but also fill the vacancies, inhibiting the diffusion of Zn through these vacancies, resulting in improvement of the corrosion resistance [14].

In the NaCl solution, the Ce Al brass is shown to have a slightly higher corrosion resistance than the As Al brass. Compared with the addition of As, the addition of Ce results in a little decrease of free corrosion potential of the brass but a significant increase of polarization resistance as shown in Fig. 1. Ce is an active element and likely to be oxygenated which leads to a little decrease of free corrosion potential of the brass, however the corrosion product layer is dense and has a much improved bonding with the matrix by it, as shown in Figs. 2 and 4a, which results in a significant increase of polarization resistance. It is likely that this dense film inhibited the diffusion of Zn atom from matrix into the solution and thus increased the corrosion resistance.
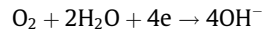
In the NaCl + NH$_4$Cl solution, the corrosion average rates of the As Al brass and Ce Al brass are very similar and are much higher than those in the NaCl solution.

As the brass is immersed into the solution with NH4$^+$, the anode and cathode reactions take place

Anode reaction :

$$Cu + nNH_3 \rightarrow Cu(NH_3)_n^{2+} + 2e \quad (n = 1, 2, 3, 4)$$
$$Cu + Cu(NH_3)_2^{2+} \rightarrow 2Cu(NH_3)^{2+} + 2e$$
$$Zn + nNH_3 \rightarrow Zn(NH_3)_n^{2+} + 2e \quad (n = 1, 2, 3, 4)$$
$$Zn + Zn(NH_3)_2^{2+} \rightarrow 2Zn(NH_3)^{2+} + 2e$$

Cathode reaction :

$$O_2 + 2H_2O + 4e \rightarrow 4OH^-$$

The reaction of $Cu + Cu(NH_3)_2^{2+} \rightarrow 2Cu(NH_3)^{2+} + 2e$ is self-catalysis process. The complex compound of $Cu(NH_3)^{2+}$ is water miscible complex.

Therefore, the majority of the corrosion products of the Ce Al brass in the NaCl + NH$_4$Cl solution are dissolved into the solution and there is no corrosion product layer to cover the matrix. As a consequence, the corrosion process can proceed continuously without any protection. For the As Al brass, besides the Zn, the majority of Cu has been released during immersing in the solution, and As cannot be inhibited the diffusion of Cu. In any case, the corrosion rate of the Ce Al brass is nearly the same as that of the As Al brass. Ce is therefore a suitable alternative to As as an alloying element in Al brass for improving the corrosion resistance.

4. Conclusions

(1) The hot-working and cold-working characters of the Ce Al brass are good, and the suitable hot-working temperature of Ce Al brass is between 973 and 1023 K.
(2) In the NaCl solution, the corrosion rate of Ce Al brass is 0.000212 mm/yr lower than that of the As Al brass.
(3) In the NaCl solution, the Ce Al brass has a 0.0818 V lower corrosion potential but a 1280.5 Ω/cm^2 higher polarization resistance than that of the As Al brass. The corrosion product layer is dense and has a much improved bonding with the matrix by it.
(4) In the NaCl + NH$_4$Cl solution, the corrosion rates of the two alloys are much higher and have nearly the same value.

Acknowledgement

References

[1] Ismail KM, Fathi AM, Badawy WA. The influence of Ni content on the stability of copper–nickel alloys in alkaline sulphate solutions. J Appl Electrochem 2004;34:823–31.
[2] Milosev I. The effect of various halide ions on the passivity of Cu, Zn and Cu–xZn alloys in borate buffer. Corros Sci 2007;49:637–53.
[3] Polunin AV, Pchelnikov AP, Losev VV, Marshakov IK. Electrochemical studies of the kinetics and mechanism of brass dezincification. Electrochim Acta 1982;27:467–75.
[4] Dinnappa RK, Mayanna SM. The dezincification of brass and its inhibition in acidic chloride and sulphate solutions. Corrosion Sci 1987;27:349–61.
[5] Kolotyrkin VA, Chervyakov VN, Pschelnikov AP, Losev VV. Electrochemical behavior of brass under conditions of stress corrosion cracking. Zashch Met 1995;31:220–3.
[6] Tromans D. Copper and zinc equilibria in concentrated ammonia solutions: relevance to stress corrosion cracking of alpha-brass. Corros Sci 1997;39:1307–19.
[7] Pickering HW. Formation of new phases during anodic dissolution of Zn-rich Cu–Zn alloys. J Electrochem Soc 1970;117:8–15.
[8] Gaden H, Kalser H, Kaesche H. A morphological study of dezincification of brass. Corros Sci 1990;30:737–9.
[9] Heidersbach R. Clarification of the mechanism of the dealloying phenomenon. Corrosion 1968;24:38–44.
[10] Heidersbach R, Verink Jr EP. Dezincification of alpha and beta brasses. Corrosion 1972;28:397–418.
[11] Gad-Allah AG, Abou-Romia MM, Badawy MW, Rehan HH. Passivity of α-brass (Cu:Zn/33:67) and its breakdown in neutral and alkaline solutions containing halide ions. J Appl Electrochem 1991;21:829–36.
[12] Horton RM. New metallographic evidence for dezincification of brass by redisposition of copper. Corrosion 1970;26:160–3.
[13] Lucey VF. The mechanism of dezincification and the effect of arsenic parts I. Brit Corros J 1965;1:9–14.
[14] Lucey VF. The mechanism of dezincification and the effect of arsenic parts II. Brit Corros J 1965;1:53–9.

[15] Chen JY, Li Z, Tang N. Corrosion behavior of tin brass containing rare earth. Trans Mater Heat Treat 2007;28:101–4 (in Chinese).

[16] Kear G, Barker BD, Stokes K, Walsh FC. Flow influenced electrochemical corrosion of nickel aluminium bronze – Part II. Anodic polarisation and derivation of the mixed potential. J Appl Electorchem 2004;34:1241–7.

[17] Schussler A, Exner HE. The corrosion of nickel–aluminium bronzes in seawater—I. Protective layer formation and the passivation mechanism. Corros Sci 1993;34:1793–802.

[18] Schussler A, Exner HE. The corrosion of nickel–aluminium bronzes in seawater—II The corrosion mechanism in the presence of sulphide pollution. Corros Sci 1993;34:1803–11.